

The Effect of Orbital Eccentricity on Gravitational Wave Background Radiation from Cosmological Binaries

Motohiro ENOKI^{1,*)}, and Masahiro NAGASHIMA^{2,3}

¹*National Astronomical Observatory of Japan, Mitaka, Tokyo, 181-8588, Japan*

²*Department of Physics, Kyoto University, Kyoto, 606-8502, Japan*

³*Faculty of Education, Nagasaki University, Nagasaki, 852-8521, Japan*

A compact binary on an eccentric orbit radiates gravitational waves (GWs) at all integer harmonics of its orbital frequency. Thus, the spectral energy distribution, the power and the timescale of GW radiation of a binary on an eccentric orbit are different from those of a binary on a circular orbit. Therefore, in order to predict spectra of gravitational wave background radiation (GWBR) from compact binaries, it is important to include the effect of orbital eccentricity of binaries. In this study, we investigate the effect of orbital eccentricity on expected GWBR from extragalactic compact binaries. For this purpose, we formulate the power spectrum of GWBR from cosmological evolving eccentric binaries. Then we apply this formulation to the case of the GWBR from supermassive black hole (SMBH) binaries in galaxy nuclei. The key to do this is correctly estimating the number density of coalescing SMBH binaries. In this study, we use a semi-analytic model of galaxy and SMBH formation. We find that the power spectrum of the GWBR from SMBH binaries on eccentric orbits is suppressed for frequencies $\lesssim 1\text{Hz}$ dependent on an assumed initial eccentricity. Our model predicts that while the overall shape and amplitude of the power spectrum depend largely on galaxy formation processes, eccentricity of binaries can affect the shape of the power spectrum for lower frequencies $\lesssim 1\text{Hz}$. Pulsar timing measurements, which can detect GW at this frequency range, would be able to constrain the effect of eccentricity on the power spectrum of the GWBR from SMBH binaries.

§1. Introduction

An ensemble of gravitational waves (GWs) from a number of inspiraling binaries of compact objects at different redshift can be observed as stochastic gravitational wave background radiation (GWBR). Resulting from mergers of their host galaxies, coalescing supermassive black hole (SMBH) binaries with mass $10^6 - 10^9 M_\odot$ emit GWs. Recent studies^{1),2)} predict that these SMBH binaries produce GWBR for frequencies $\sim 1\text{n} - 1\mu\text{Hz}$. In the frequency range $0.1\text{m} - 10\text{mHz}$, it is expected that extragalactic close binaries of white dwarfs are dominant sources of GWBR.³⁾

GWs at frequencies $1\text{n} - 100\text{nHz}$ can be detected by pulsar timing measurements.⁴⁾ Thereby we will be able to detect the GWBR from SMBH binaries directly. Recently, Jenet et al.⁵⁾ developed a new method for detecting GWBR using multiple pulsar timing data. To the case of the Parkes Pulsar Timing Array (PPTA) project^{6) **)}, their results showed that regular timing observations of 20 pulsars with timing accuracy of 100ns would be able to make a direct detection of the predicted levels of the GWBR from SMBH binaries within 5 years.⁵⁾

In previous studies^{1),2)} of GWBR from SMBH binaries, it is assumed that all

^{*}) E-mail:enoki.motohiro@nao.ac.jp

^{**)} See <http://www.atnf.csiro.au/research/pulsar/array/>

binaries are on circular orbits. However, binary orbits are generally eccentric. Before entering into the GW emitting regime, a SMBH binary evolves owing to dynamical interaction with field stars in the center of its host galaxy. Mikkola and Valtonen⁷⁾ constructed approximate expressions between the energy and angular momentum transfer rates for a heavy binary and a surrounding field of light stars, and showed that the semi-major axis decreases and the eccentricity increases owing to dynamical friction. Fukushige et al.⁸⁾ investigated the evolution of a SMBH binary in uniformly distributed field stars and found that the dynamical friction on the eccentric binary is the most effective at the apocenter where orbital velocity is minimum and thus the eccentricity increases. Iwasawa et al.⁹⁾ performed N -body simulations of dynamical evolution of triple SMBHs (a binary of SMBHs and a single SMBH) systems in galactic nuclei and showed that the eccentricity of the SMBH binary reached $e > 0.9$ at the GW emission regime. They found that both the Kozai mechanism and the thermalization of eccentricity due to the strong binary-single SMBH interaction drive the increase of the orbital eccentricity. Matsubayashi et al.¹⁰⁾ investigated orbital evolution of intermediate mass black hole (IMBH)-SMBH systems in galactic centers, using N -body simulations. They found that the eccentricity approaches to unity ($e > 0.8$) and the IMBH can coalesce the SMBH quickly as a result of GW emission. Armitage and Natarajan¹¹⁾ studied the evolution of the SMBH binary eccentricity which is excited by the interaction between the binary and circumbinary gas disk. They estimated a typical eccentricity at one week prior to coalescence $e \sim 0.01$. Higher eccentricity ($e \sim 0.1$) are possible for the case of extreme-mass ratio binary.

An eccentric binary emits GWs at all integer harmonics of the orbital frequency.^{12),13)} Thus, the spectral energy distribution (SED) is different from that of a binary on a circular orbit, even if masses and semi-major axis of both binaries are the same. For larger eccentricity, radiation of higher harmonics is stronger and thus the peak of SED shifts toward higher frequency. Moreover, orbital evolution of a binary due to GW radiation depends strongly on its eccentricity. As a result, the power of GW radiation of an eccentric binary is larger than that of a circular binary and the timescale of GW radiation of an eccentric binary is shorter than that of a circular binary. Therefore, in order to predict the power spectrum of GWBR from compact binaries, it is necessary to take account of orbital eccentricities of binaries.

In this study, we investigate the effect of orbital eccentricity on expected GWBR from extragalactic compact binaries. At first, we formulate the power spectrum of GWBR from cosmological eccentric binaries, taking into account eccentricity evolution. In order to formulate the power spectrum, we adopt a simple relationship between the power spectrum of the GWBR produced by cosmological GW sources, the total time-integrated energy spectrum of individual sources, and the comoving number density of GW sources found by Phinney.¹⁴⁾ Next, we apply this formulation to the case of the GWBR from coalescing SMBH binaries. In order to estimate the number density of SMBH binaries, we use a semi-analytic (SA) model¹⁶⁾ in which SMBH formation is incorporated into galaxy formation.¹⁵⁾

The paper is organized as follows: in section 2 we briefly review GWs emission of a binary on an eccentric orbit; in section 3 we formulate the power spectrum of GWBR from cosmological compact binaries on eccentric orbits; in section 4 we

present the power spectrum of the GWBR from eccentric SMBH binaries; in section 5 we provide summary and conclusions.

§2. GWs from a binary on eccentric orbit

Here we briefly review GWs from a binary on an eccentric orbit and evolution of a binary due to GW emission in the weak field and slow motion limit.^{12),13)}

The total power of the GW emission of a Keplerian binary with two point masses M_1 and M_2 , orbital frequency f_p and orbital eccentricity e is

$$L_{\text{GW}}(M_1, M_2, f_p, e) = L_{\text{GW,circ}}(M_1, M_2, f_p)F(e), \quad (2.1)$$

where

$$\begin{aligned} L_{\text{GW,circ}}(M_1, M_2, f_p) &= \frac{32}{5} \frac{G^{7/3}}{c^5} M_{\text{chirp}}^{10/3} (2\pi f_p)^{10/3} \\ &= 4.7 \times 10^{48} \left(\frac{M_{\text{chirp}}}{10^8 M_\odot} \right)^{10/3} \left(\frac{2f_p}{10^{-7} \text{ Hz}} \right)^{10/3} \text{ erg}, \end{aligned} \quad (2.2)$$

and

$$F(e) \equiv \frac{1 + 73e^2/24 + 37e^4/96}{(1 - e^2)^{7/2}}. \quad (2.3)$$

$L_{\text{GW,circ}}(M_1, M_2, f_p)$ is the total power from a binary on a circular orbit with masses M_1 and M_2 , and orbital frequency f_p , which is the reciprocal of the proper rest-frame period of the binary. G is the gravitational constant and c is the speed of light. $M_{\text{chirp}} \equiv [M_1 M_2 (M_1 + M_2)^{-1/3}]^{3/5}$ is the chirp mass of the system. The total power of GW emission is distributed into each the power of the n th harmonic of the orbital frequency, $L_{\text{GW,circ}}(M_1, M_2, f_p)g(n, e)$, with rest-frame GW frequency, $f_r = nf_p$. $g(n, e)$ is GW frequency distribution function expressed as

$$\begin{aligned} g(n, e) &\equiv \frac{n^4}{32} \left\{ \left[J_{n-2}(ne) - 2eJ_{n-1}(ne) + \frac{2}{n}J_n(ne) + 2eJ_{n+1}(ne) - J_{n+2}(ne) \right]^2 \right. \\ &\quad \left. + (1 - e^2) [J_{n-2}(ne) - 2eJ_n(ne) + J_{n+2}(ne)]^2 + \frac{4}{3n^2} [J_n(ne)]^2 \right\} \end{aligned} \quad (2.4)$$

where J_n is the n th order Bessel function. It can be shown that

$$\sum_{n=1}^{\infty} g(n, e) = F(e). \quad (2.5)$$

For the case of a circular orbit (i.e., $e = 0$), $g(n, 0) = 0$ except for $n = 2$ and $g(2, 0) = 1$. The SED of gravitational radiation is given by

$$L_{f_r}(e, t_p) = L_{\text{GW,circ}}(f_p) \sum_{n=1}^{\infty} g(n, e) \delta(f_r - nf_p). \quad (2.6)$$

Here, t_p is the time at the orbital frequency f_p and $\delta(x)$ is Dirac's delta function.

The timescale emitting GW of a binary measured in the rest-frame is

$$\tau_{\text{GW}} \equiv f_p \frac{dt_p}{df_p}. \quad (2.7)$$

This timescale is given by

$$\tau_{\text{GW}}(M_1, M_2, f_p, e) = \frac{\tau_{\text{GW,circ}}(M_1, M_2, f_p)}{F(e)} \quad (2.8)$$

where $\tau_{\text{GW,circ}}(M_1, M_2, f_p)$ is the timescale emitting GW for a binary in a circular orbit. This timescale is given by

$$\begin{aligned} \tau_{\text{GW,circ}}(M_1, M_2, f_p) &= \frac{5}{96} \left(\frac{c^3}{GM_{\text{chirp}}} \right)^{5/3} (2\pi f_p)^{-8/3} \\ &= 1.2 \times 10^4 \left(\frac{M_{\text{chirp}}}{10^8 M_{\odot}} \right)^{-5/3} \left(\frac{2f_p}{10^{-7} \text{ Hz}} \right)^{-8/3} \text{ yr.} \end{aligned} \quad (2.9)$$

As a result of the GW emission, the energy and angular momentum of a binary are lost and the orbit of the binary is circularized. The evolutions of semi-major axis a and eccentricity e are given as follows,

$$\begin{aligned} \frac{da}{dt} &= -\frac{64}{5} \frac{G^3 M_1 M_2 M_{\text{tot}}}{c^5 a^3 (1-e^2)^{7/2}} \left(1 + \frac{73}{24} e^2 + \frac{37}{96} e^4 \right) \\ &= -\frac{64}{5} \frac{G^3 M_1 M_2 M_{\text{tot}}}{c^5 a^3} F(e), \end{aligned} \quad (2.10)$$

and

$$\frac{de}{dt} = -\frac{304}{15} \frac{G^3 M_1 M_2 M_{\text{tot}}}{c^5 a^4 (1-e^2)^{5/2}} e \left(1 + \frac{121}{304} e^2 \right), \quad (2.11)$$

where $M_{\text{tot}} \equiv M_1 + M_2$. Starting from a given orbit with parameters a_0 and e_0 , Equations (2.10) and (2.11) give the relation between a and e given by

$$\frac{a}{a_0} = \frac{1 - e_0^2}{1 - e^2} \left(\frac{e}{e_0} \right)^{\frac{12}{19}} \left[\frac{1 + \frac{121}{304} e^2}{1 + \frac{121}{304} e_0^2} \right]^{\frac{870}{2299}}. \quad (2.12)$$

Since $a^3 = GM_{\text{tot}}/(2\pi f_p)^2$, the relation between the orbital frequency and eccentricity is described as

$$\frac{f_p}{f_{p,0}} = \left\{ \frac{1 - e_0^2}{1 - e^2} \left(\frac{e}{e_0} \right)^{\frac{12}{19}} \left[\frac{1 + \frac{121}{304} e^2}{1 + \frac{121}{304} e_0^2} \right]^{\frac{870}{2299}} \right\}^{-3/2}, \quad (2.13)$$

where $f_{p,0}$ is the initial orbital frequency. In Fig. 1, we plot the evolution of eccentricity as a function of orbital frequency $f_p/f_{p,0}$.

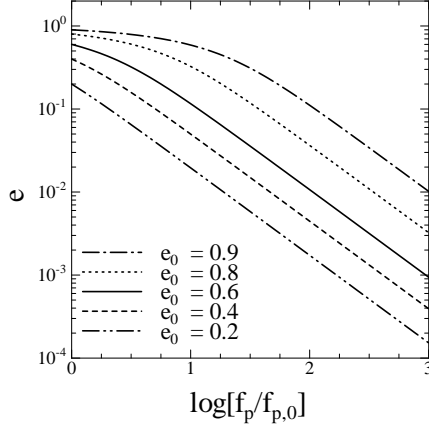


Fig. 1. Evolution of eccentricity, $e = e(f_p/f_{p,0}, e_0)$ as a function of orbital frequency $f_p/f_{p,0}$ for $e_0 = 0.2, 0.4, 0.6, 0.8$ and 0.9 .

§3. GWBR from binaries on eccentric orbits

3.1. Characteristic amplitude of GWBR spectrum

In any homogeneous and isotropic universe, the present-day GWBR energy density $\rho_{\text{GW}}c^2$ must be equal to sum of the energy densities radiated at each redshift z , divided by $(1+z)$ to account for the redshifting as follows,

$$\rho_{\text{GW}}c^2 = \int_0^\infty \int_0^\infty n_c(z) \frac{1}{1+z} \frac{dE_{\text{GW}}}{df_r} df_r dz \quad (3.1)$$

$$= \int_0^\infty \int_0^\infty n_c(z) \frac{1}{1+z} f_r \frac{dE_{\text{GW}}}{df_r} dz \frac{df}{f}. \quad (3.2)$$

Here, $n_c(z)dz$ is the comoving number density of GW sources at redshift $z \sim z + dz$. f_r is the GW frequency in a source's *rest-frame*, and f is the the GW frequency in the *observer-frame*, so $f_r = f(1+z)$.

$$\frac{dE_{\text{GW}}}{df_r} df_r \quad (3.3)$$

is the total energy emitted in GWs between frequency f_r and $f_r + df_r$. This energy is measured in the source's rest-frame, and is integrated over all solid angles and over the entire radiating lifetime of the source. Then the total present day energy density in GWs is

$$\rho_{\text{GW}}c^2 \equiv \int_0^\infty \frac{\pi c^2}{4 G} f^2 h_c^2(\ln f) \frac{df}{f}, \quad (3.4)$$

where $h_c(\ln f)$ is the characteristic amplitude of the GWBR power spectrum over a logarithmic frequency interval $d \ln f = df/f$. Therefore, we find

$$h_c^2(\ln f) = \frac{4G}{\pi c^2 f^2} \int_0^\infty n_c(z) \frac{1}{1+z} \left(f_r \frac{dE_{\text{GW}}}{df_r} \right) \Big|_{f_r=f(1+z)} dz,$$

$$= \frac{4G}{\pi c^2 f} \int_0^\infty n_c(z) \left(\frac{dE_{\text{GW}}}{df_r} \right) \Big|_{f_r=f(1+z)} dz. \quad (3.5)$$

If GW sources are coalescing binaries, the characteristic amplitude is given by

$$h_c^2(\ln f) = \frac{4G}{\pi c^2 f} \int dM_1 dM_2 dz n_c(M_1, M_2, z) \left(\frac{dE_{\text{GW}}(M_1, M_2)}{df_r} \right) \Big|_{f_r=f(1+z)} \quad (3.6)$$

where $n_c(M_1, M_2, z) dM_1 dM_2 dz$ is the comoving number density of coalescing binaries with mass $M_1 \sim M_1 + dM_1$ and $M_2 \sim M_2 + dM_2$ at $z \sim z + dz$.

Note that equation (3.5) assumes that the timescale of GW emission is much shorter than the Hubble time. This relationship between the power spectrum of the GWBR produced by cosmological distribution of discrete GW sources and the total time-integrated energy spectrum of an individual source derived by Phinney.¹⁴⁾

3.2. Total energy emitted in GWs

The total energy of GW radiation with lifetime t_{life} is

$$E_{\text{GW}} = \int_0^{t_{\text{life}}} L_{\text{GW}}(t_p) dt_p \quad (3.7)$$

$$= \int_0^{t_{\text{life}}} \int L_{f_r}(t_p) df_r dt_p, \quad (3.8)$$

where $L_{\text{GW}}(t_p)$ is the power of GW emission and $L_{f_r}(t_p)$ is the SED of GW emission. Then,

$$\frac{dE_{\text{GW}}}{df_r} = \int_0^{t_{\text{life}}} L_{f_r}(t_p) dt_p. \quad (3.9)$$

Therefore, given the number density and SED of GW sources, we can calculate the amplitude of the GWBR power spectrum.

3.3. Characteristic amplitude of the GWBR spectrum from eccentric binaries

For a Keplerian binary with two point masses M_1 and M_2 and orbital eccentricity e , the SED of GW radiation is given by equation (2.6). From equations (2.6), (2.7) and (3.9), we obtain

$$\begin{aligned} \frac{dE_{\text{GW}}}{df_r} &= \int L_{\text{GW,circ}}(f_p) \frac{dt_p}{df_p} \sum_{n=1}^{\infty} g(n, e) \delta(f_r - n f_p) df_p \\ &= \sum_{n=1}^{\infty} \left[L_{\text{GW,circ}}(f_p) \frac{\tau_{\text{GW}}(f_p, e)}{n f_p} g(n, e) \right] \Big|_{f_p=f_r/n}. \end{aligned} \quad (3.10)$$

Thus, from equations (3.6) and (3.10), the power spectrum of GWBR from binaries on eccentric orbits is described as

$$\begin{aligned} h_c^2(\ln f) &= \frac{4G}{\pi c^2 f} \int dM_1 dM_2 dz n_c(M_1, M_2, z) \sum_{n=1}^{\infty} \left[L_{\text{GW,circ}}(f_p) \frac{\tau_{\text{GW}}(f_p, e)}{n f_p} g(n, e) \right] \Big|_{f_p=f(1+z)/n} \\ &= \frac{4\pi c^3}{3} \int dM_1 dM_2 dz n_c(M_1, M_2, z) (1+z)^{-1/3} \left(\frac{GM_{\text{chirp}}}{c^3} \right)^{5/3} (\pi f)^{-4/3} \Phi \end{aligned} \quad (3.11)$$

where

$$\Phi \equiv \sum_{n=1}^{\infty} \Phi_n, \quad (3.12)$$

and

$$\Phi_n \equiv \left(\frac{2}{n} \right)^{2/3} \frac{g(n, e)}{F(e)}. \quad (3.13)$$

The left panel of Fig. 2 shows $g(n, e)$ as a function of eccentricity, e , and the right panel shows Φ and Φ_n as a function of e .

Here we note that the eccentricity, e , is a function of the orbital frequency $f_p/f_{p,0}$ (see equation [2.13] and Fig. 1). Therefore, $e = e(f_p/f_{p,0}, e_0) = e(f_r/nf_{p,0}, e_0) = e[f(1+z)/nf_{p,0}, e_0]$. Hence, Φ depends on f , $f_{p,0}$, e_0 and z . Since SMBH binaries have various initial eccentricities, the number density in the equation (3.11) should be $n_c(M_1, M_2, e_0, z)$ and be also integrated over e_0 . However, in this paper, we assume that all binaries have the same initial eccentricity e_0 for simplicity. If all binaries are circular (i.e., $e_0 = 0$), $\Phi_2 = 1$ and $\Phi_n = 0$ for $n \neq 2$. Thus, $h_c \propto f^{-2/3}$ for $e_0 = 0$. On the other hand, for $e_0 \neq 0$, Φ depends on f , and h_c is not proportional to $f^{-2/3}$. Therefore, Φ indicates the strength of the effect of orbital eccentricity on the GWBR power spectrum. In the left panel of Fig. 3, we plot Φ as a function of rest-frame GW frequency $f_r/f_{p,0}$ for some initial eccentricities. In the right panel of Fig. 3, we plot Φ_n with $e_0 = 0.8$ as a function of $f_r/f_{p,0}$ for some harmonics. Owing to the harmonics radiation, the power spectrum is suppressed at lower frequencies $f_r/f_{p,0} \lesssim 10$ and is amplified at intermediate frequencies $10 \lesssim f_r/f_{p,0} \lesssim 100$. For larger frequencies $100 \lesssim f_r/f_{p,0}$, the main contributors to the power spectrum is circular binaries, which evolve from eccentric binaries and radiate only the $n = 2$ mode.

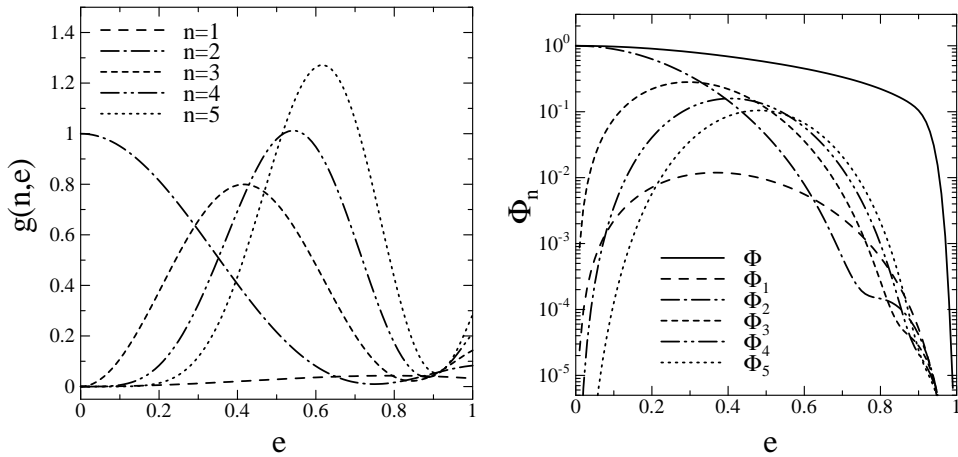


Fig. 2. Left panel: $g(n, e)$ as a function of e for $n = 1, 2, 3, 4$ and 5. Right panel: Φ and Φ_n for $n = 1, 2, 3, 4$ and 5 as a function of e .

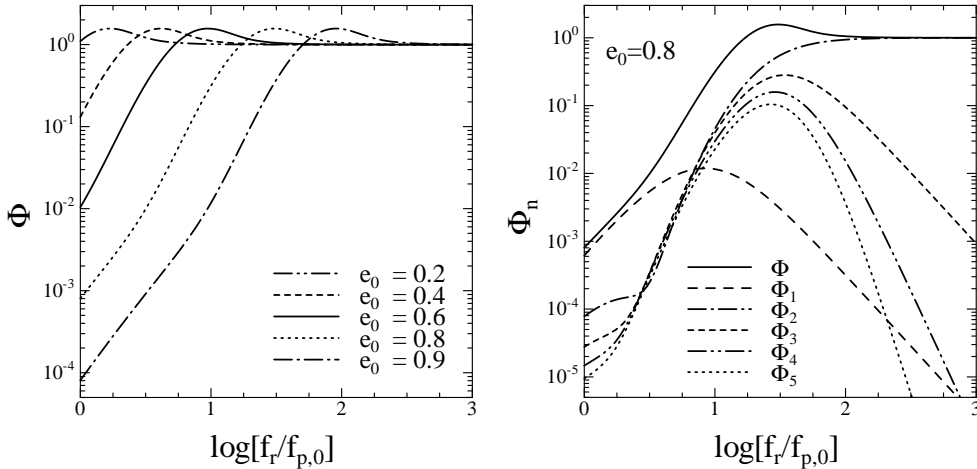


Fig. 3. Strength of the effect of orbital eccentricity on GWBR power spectra. Left panel: $\Phi = \Phi(f_r/f_{p,0}, e_0)$ as a function of $f_r/f_{p,0}$ for $e_0 = 0.2, 0.4, 0.6, 0.8$ and 0.9 . Right panel: Φ_n with $e_0 = 0.8$ as a function of $f_r/f_{p,0}$ for $n = 1, 2, 3, 4$ and 5 . Φ for $e_0 = 0.8$ also is shown.

§4. Power spectrum of the GWBR from eccentric SMBH binaries

4.1. An unified semi-analytic model of galaxy and SMBH formation

In order to predict the power spectrum of the GWBR from coalescing SMBH binaries, we must estimate the number density of coalescing SMBH binaries. To do this, we use a semi-analytic (SA) model¹⁶⁾ in which SMBH formation is incorporated into galaxy formation.¹⁵⁾

In the standard hierarchical structure formation scenario in a cold dark matter (CDM) universe, dark-matter halos (*dark halos*) cluster gravitationally and merge together. In each of merged dark halos, a galaxy is formed as a result of radiative gas cooling. In each galaxy, star formation and supernova feedback occur. Several galaxies in a common dark halo sometimes merge together and a more massive galaxy is assembled. When galaxies merge, SMBHs in centers of galaxies sink toward the center of the new merged galaxy and form a SMBH binary subsequently. If the binary loses enough energy and angular momentum, it will evolve to the GW emitting regime and begin inspiraling, eventually coalesces with a GW burst.

In SA models, merging histories of dark halos are realized using a Monte-Carlo algorithm and evolution of baryonic components within dark halos is calculated using simple analytic models for gas cooling, star formation, supernova feedback, galaxy merging and other processes. SA models have successfully reproduced a variety of observed features of galaxies, such as their luminosity functions and gas fraction in disk galaxies. In our SMBH formation incorporated SA-model,¹⁶⁾ it is assumed that SMBHs grow by coalescence of two or more SMBHs when their host galaxies merge. We also assume that during a major merger, some fraction of the cold gas that is proportional to the total mass of stars newly formed at starburst is accreted onto the newly formed SMBH, and that this gas fueling leads quasar activities. Thus, SMBHs

also grow by accretion of cold gas. Our SA model reproduces not only observational features of galaxies¹⁵⁾ but also the observed SMBH mass function at present and the quasar luminosity functions at different redshifts.¹⁶⁾ Using this SA-model, Enoki et al. estimated the amplitude of GWBR from inspiraling SMBH binaries on circular orbits and the event rate of GW bursts due to SMBH binary coalescing.¹⁾

In this study, the adopted cosmological model is a low-density, spatially flat cold dark matter (Λ CDM) universe with the present density parameter, $\Omega_m = 0.3$, the cosmological constant, $\Omega_\Lambda = 0.7$, and the Hubble constant $h = 0.7$ ($h \equiv H_0/100 \text{ km s}^{-1} \text{ Mpc}^{-1}$). Detailed model description and model parameters are given in Nagashima et al.¹⁵⁾ and Enoki et al.^{1), 16)}

4.2. Maximum Orbital Frequency

Putting the number density of coalescing SMBH binaries, $n_c(M_1, M_2, z)dM_1dM_2dz$ into the equation (3.11), we can calculate the power spectrum of the GWBR from SMBH coalescing SMBH binaries. Here, we introduce the cut-off orbital frequency $f_{p,\max}$.¹⁾ As a binary evolves with time owing to GW radiation, the frequency becomes higher. We assume that the binary orbit is quasi-stationary until the radius equals to $3R_S$, where R_S is the Schwarzschild radius : the radius of the innermost stable circular orbit (ISCO) for a particle around a non-rotating black hole. Then the maximum orbital frequency $f_{p,\max}$ is

$$\begin{aligned} f_{p,\max}(M_1, M_2) &= \frac{c^3}{6^{3/2} 2\pi GM_1} \left(1 + \frac{M_2}{M_1}\right)^{1/2} \\ &= 2.2 \times 10^{-5} \left(\frac{M_1}{10^8 M_\odot}\right)^{-1} \left(1 + \frac{M_2}{M_1}\right)^{1/2} \text{ Hz}, \end{aligned} \quad (4.1)$$

where M_1 and M_2 are SMBH masses ($M_1 > M_2$). Then, in equation (2.6), we replace $L_{\text{GW,circ}}(f_p)$ by $L_{\text{GW,circ}}(f_p)\theta(f_{p,\max} - f_p)$. Here, $\theta(x)$ is the step function. Therefore, Φ_n becomes

$$\Phi_n = \left(\frac{2}{n}\right)^{2/3} \frac{g(n, e)}{F(e)} \theta(f_{p,\max} - f(1+z)/n). \quad (4.2)$$

If this cut-off does not exits, $h_c \propto f^{-2/3}$ over $f \gtrsim 2f_{p,\max}$.

4.3. Results

In Fig. 4, we plot power spectra of GWBR, h_c , from SMBH binaries for various initial eccentricities. e_0 and $f_{p,0}$ are given at $f_{p,0}/f_{p,\max} = 10^{-3}$ ($a = 300R_S$). This figure shows that power spectra at the frequency measured by pulsar timing ($f \sim 1\text{Hz}$) are suppressed as a result of harmonics radiation, especially for $e_0 \gtrsim 0.4$. The slope of the spectrum changes at $f \sim 1\mu\text{Hz}$ owing to lack of power associated with the upper limit frequency, $f_{p,\max}$.

In the left panel of Fig. 5, we show some harmonics of the GWBR power spectrum from SMBH binaries for $e_0 = 0.8$ and $f_{p,0}/f_{p,\max} = 10^{-3}$. As with the right panel of Fig. 3, in the lower frequency range $f \lesssim 1\text{Hz}$, the $n = 1$ mode is dominant

and in the higher frequency range $f \gtrsim 0.1\mu\text{Hz}$, the $n = 2$ mode is dominant. Therefore, in this frequency range, GWs from circular binaries are dominant. In the right panel of Fig. 5, we plot power spectra of GWBR from SMBH binaries for $e_0 = 0.8$ in different initial orbital frequencies for $f_{p,0}/f_{p,\text{max}} = 5^{-3}, 10^{-3}$ and 20^{-3} . Because $a \propto f_p^{-2/3}$, these correspond to $a = 75R_S, 300R_S$ and $600R_S$, respectively. This figure indicates that the shape of the power spectrum in the low frequency range depends strongly on $f_{p,0}/f_{p,\text{max}}$.

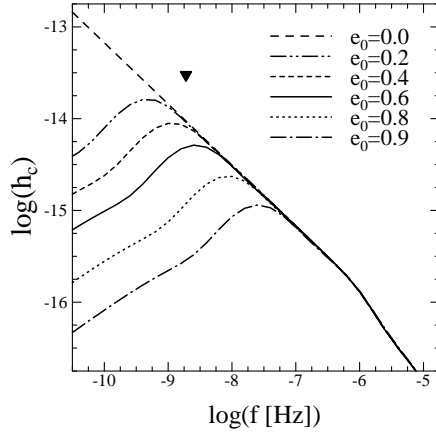


Fig. 4. Characteristic amplitudes of GWBR power spectra over a logarithmic frequency interval, $h_c(\ln f)$, from SMBH binaries with $f_{p,0}/f_{p,\text{max}} = 10^{-3}$ for $e_0 = 0.0, 0.2, 0.4, 0.6, 0.8$ and 0.9 . The filled reverse triangle shows the current limit from pulsar timing measurements.¹⁷⁾

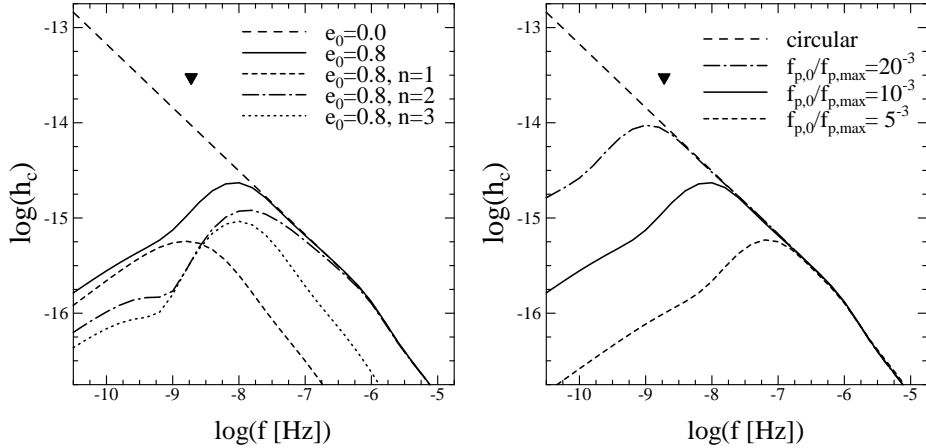


Fig. 5. Power spectra of GWBR from SMBH binaries for $e_0 = 0.8$. Left panel: Some harmonics of GWBR spectrum for $n = 1, 2$ and 3 . The initial orbital frequency is $f_{p,0}/f_{p,\text{max}} = 10^{-3}$. Right panel: Power spectra of GWBR in different initial orbital frequencies for $f_{p,0}/f_{p,\text{max}} = 5^{-3}, 10^{-3}$ and 20^{-3} . In each panel, we also plot the power spectrum of GWBR from circular binaries (dashed-line) and the current limit from pulsar timing measurements (filled reverse triangle).¹⁷⁾

The present day energy density parameter of GWBR over a logarithmic fre-

quency interval $d \ln f = df/f$ is given by

$$\Omega_{\text{GW}}(\ln f) = \frac{2\pi^2}{3H_0^2} f^2 h_c^2(\ln f). \quad (4.3)$$

In Fig. 6, we plot $\Omega_{\text{GW}}(\ln f)$ from SMBH binaries for $e_0 = 0.8$ and $f_{p,0}/f_{p,\text{max}} = 10^{-3}$, and for $e_0 = 0$ in different total SMBHs mass intervals ($M_{\text{tot}} = M_1 + M_2$). The main contribution for the energy density is from binaries with total masses $M_{\text{tot}} = 10^7 - 10^{10} M_{\odot}$. In the lower frequency range ($f \lesssim 0.1 \text{ nHz}$), which can be measured by pulsar timing, GWs from binaries with masses $M_{\text{tot}} \geq 10^9 M_{\odot}$ are dominant. As with the left panel of Fig. 3, Fig. 6 shows suppressions and amplifications of energy density parameters of each SMBH mass interval due to the harmonics radiation.

Pulsar timing measurements will allow GWs with frequencies about $1 \text{ nHz} - 100 \text{ nHz}$ to be detected. Under the assumption $h_c \propto f^{-2/3}$, the completed PPTA data-set (20 pulsar with an rms timing residual of 100 ns over 5 years) could potentially provide limits on the level of GWBR from SMBH binaries, $\Omega_{\text{GW}} = 5.5 \times 10^{-10}$ at $f = 10^{-7.5} \text{ Hz}$ (1 yr^{-1}), $\Omega_{\text{GW}} = 1.3 \times 10^{-10}$ at $f = 10^{-8.4} \text{ Hz}$ ($1/8 \text{ yr}^{-1}$) and $\Omega_{\text{GW}} = 7.3 \times 10^{-11}$ at $f = 10^{-8.8} \text{ Hz}$ ($1/20 \text{ yr}^{-1}$).¹⁸⁾ In Fig. 6, we also plot the potential future limits. These limits are well under the predicted energy density of GWBR from SMBH binaries for $e_0 = 0$, ($h_c \propto f^{-2/3}$). Therefore, the full PPTA data-set would be able to constrain the effect of eccentricity on the GWBR from SMBH binaries.

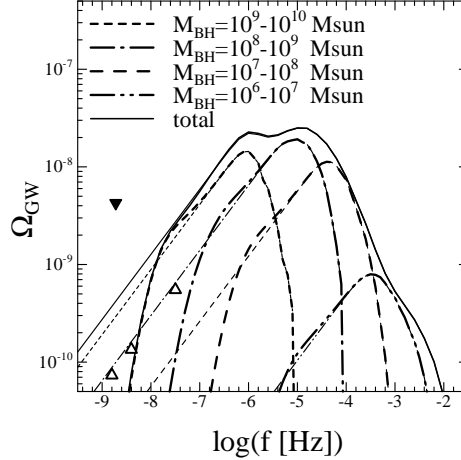


Fig. 6. Energy density parameters of GWBR over a logarithmic frequency interval $\Omega_{\text{GW}}(\ln f)$ in different total mass intervals. Thick lines show the results for $e_0 = 0.8$ and $f_{p,0}/f_{p,\text{max}} = 10^{-3}$, and thin lines show the results for $e_0 = 0$. The filled reverse triangle shows the current limit from pulsar timing measurements.¹⁷⁾ Triangles indicate the potential future lower limits from the full PPTA data-set for the case of $h_c \propto f^{-2/3}$.¹⁸⁾

4.4. Effects of galaxy formation processes on GWBR from SMBH binaries

The number density of coalescing SMBH binaries with mass $M_1 \sim M_1 + dM_1$ and $M_2 \sim M_2 + dM_2$ at $z \sim z + dz$, $n_c(M_1, M_2, z) dM_1 dM_2 dz$, depends on galaxy for-

mation processes. In our SA-model, the dominant mass growth process of SMBHs is the accretion of cold gas, which is also the material for stars.¹⁾ Thus, $n_c(M_1, M_2, z)$ depends largely on star formation related processes. Here, we show how the star formation time scale and the strength of supernova feedback affect the power spectrum of the GWBR from SMBH binaries.

In our SA-model, the star formation rate (SFR) of a galaxy is assumed by $\dot{M}_* = M_{\text{cold}}/\tau_*$, where M_{cold} is the mass of the cold gas and τ_* is the time scale of star formation. We assume $\tau_* = \tau_*^0 (V_{\text{circ}}/300 \text{ km s}^{-1})^{\alpha_*}$, where V_{circ} is the circular velocity of the galaxy. The free parameters τ_*^0 and α_* are chosen to match the observed mass fraction of cold gas in the disks of spiral galaxies. With star formation, supernovae occur and heat up the surrounding cold gas to the hot gas phase (supernova feedback). The reheating rate is given by $\dot{M}_{\text{reheat}} = \beta(V_{\text{circ}})\dot{M}_*$, where $\beta(V_{\text{circ}}) = (V_{\text{hot}}/V_{\text{circ}})^{\alpha_{\text{hot}}}$. The free parameters V_{hot} and α_{hot} are determined by matching the observed local luminosity function of galaxies. In the previous our study¹⁾ and previous subsection in this paper, we adopted $\tau_*^0 = 1.5 \text{ Gyr}$, $\alpha_* = -2$, $V_{\text{hot}} = 280 \text{ km s}^{-1}$ and $\alpha_{\text{hot}} = 2.5$ as fiducial values.

The left panel of Fig. 7 shows power spectra of GWBR from SMBH binaries for various star formation time scales, τ_*^0 . Other parameters are not changed. For large τ_*^0 , the SFR is low and thus a large amount of the cold gas remains in each galaxy. Thus, the masses of SMBHs become large. Therefore, the amplitude of the power spectrum of the GWBR become large. Moreover, the slope changing point moves to lower frequency because the upper limit frequency, $f_{p,\text{max}}$, become small. The right panel of Fig. 7 shows power spectra of GWBR from SMBH binaries for various supernovae feedback strength, V_{hot} . Other parameters are not changed. In the case of no supernovae feedback ($V_{\text{hot}} = 0 \text{ km s}^{-1}$), the cold gas is not heated up to hot gas. Thus, a large amount of cold gas remains in each galaxy and the masses of SMBHs become large. On the contrary, for the large V_{hot} case, the cold gas is much heated up and thus the masses of SMBH become small. Both panels of Fig. 7 indicate that although the shape of the power spectrum of the GWBR from SMBH binaries is affected by eccentricity of binaries for low frequencies, $f \lesssim 1 \text{ nHz}$, the shape of the power spectrum for higher frequencies and the overall amplitude depend largely on galaxy formation processes.

We note that the purpose of this subsection is to show the importance of galaxy formation processes on the growth of SMBHs and the GWBR from SMBH binaries. Therefore, in this subsection, we present cases for *extreme parameter values*. Results of models with these parameters cannot reproduce observational results, such as galaxy luminosity functions and the present SMBH mass function, at all. In Fig. 8, we plot SMBH mass functions at $z = 0$. Only the model with fiducial values is consistent with the observation obtained by Salucci et al.¹⁹⁾

§5. Summary and Conclusions

In this study, we have investigated how orbital eccentricities of binaries affect power spectra of GWBR from extragalactic compact binaries. A compact binary on an eccentric orbit radiates GWs at all integer harmonics of its orbital frequency.

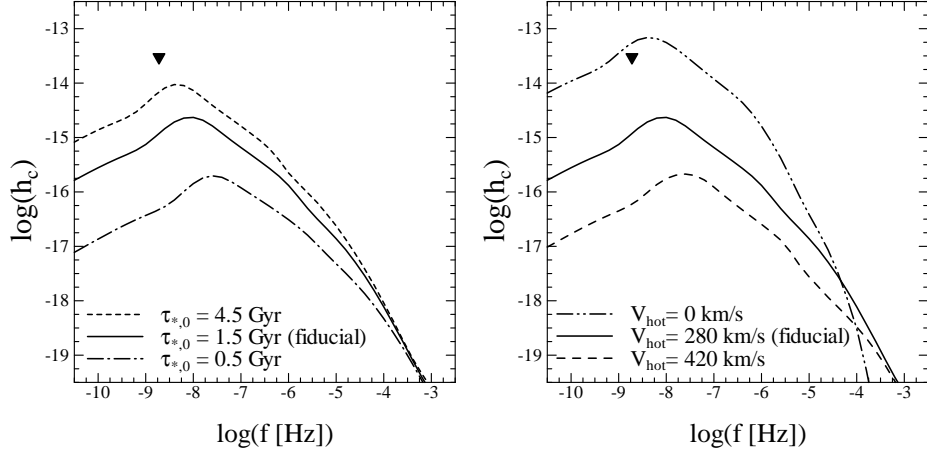


Fig. 7. Effects of galaxy formation processes on power spectrum of GWBR from SMBH binaries with $e_0 = 0.8$ and $f_{p,0}/f_{p,\max} = 10^{-3}$. Left panel: For different star formation time scales, $\tau_{*,0} = 0.5, 1.5$ and 4.5 Gyr. $\tau_{*,0} = 1.5$ Gyr is the fiducial value. Right panel: For different supernovae feedback strength, $V_{\text{hot}} = 0, 280$ and 420 km s^{-1} . $V_{\text{hot}} = 280$ km s^{-1} is the fiducial value. The case of $V_{\text{hot}} = 0$ km s^{-1} corresponds to no supernova feedback. In each panel, we also plot the current limit from pulsar timing measurements (filled reverse triangle).¹⁷⁾

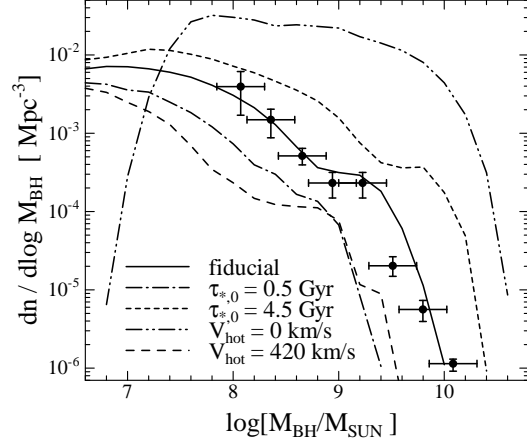


Fig. 8. SMBH mass functions of models at $z = 0$. The solid line indicates the result of the model with fiducial values, $\tau_{*,0} = 1.5$ Gyr and $V_{\text{hot}} = 280$ km s^{-1} . The symbols with error bars are the present mass function obtained by Salucci et al.¹⁹⁾

Owing to this harmonics radiation, the SED, the power and the timescale of GW emission of a binary on an eccentric orbit are different from those of a binary on a circular orbit. Therefore, at first, we have formulated the power spectrum of GWBR from cosmological compact binaries on eccentric orbits. Then using the formulation and our SA-model for galaxy and SMBH formation, we have calculated power spectra of GWBR from coalescing SMBH binaries on eccentric orbits.

Resultant power spectra of the GWBR from SMBH binaries on eccentric orbits are suppressed owing to the harmonics radiation for lower frequencies $f \lesssim 1\text{Hz}$. The

degree of the suppression depends strongly on initial eccentricities. In this paper, for simplicity, we have assumed that all binaries have a single initial eccentricity. Our study suggests that the research about the initial eccentricity distribution is very important and essential for the investigation of the power spectrum of GWBR from compact binaries.

Since the number density of coalescing SMBH binaries is determined by galaxy formation processes, the power spectrum of the GWBR from SMBH binaries depends largely on these processes, especially star formation related processes, which regulate the amount of cold gas accreted onto SMBHs. Our model prediction shows that the overall shape and amplitude of the power spectrum of the GWBR from coalescing SMBH binaries depend on galaxy formation processes. However, for low frequencies ($f \lesssim 1\text{Hz}$), the shape of the power spectrum of the GWBR depends also on the initial eccentricity. Since the pulsar timing measurements can potentially provide limits on the level of GWBR with frequencies $f \sim 1\text{nHz} - 100\text{nHz}$, the pulsar timing observations such as PPTA project would be able to constrain not only the number density of coalescing SMBH binaries but also the effect of orbital eccentricity on the GWBR from SMBH binaries.

Acknowledgements

We thank Dr. K. T. Inoue for useful suggestion. Numerical computations in this work were partly carried out at the Astronomy Data Center of the National Astronomical Observatory of Japan. This work was supported in part by a Nagasaki University president's Fund grant.

References

- 1) M. Enoki, K. T. Inoue, M. Nagashima and N. Sugiyama, *Astrophys. J.* **615** (2004), 19.
- 2) M. Rajagopal and R. Romani, *Astrophys. J.* **446** (1995), 543.
A. H. Jaffe and D. C. Backer, *Astrophys. J.* **583** (2003), 616.
- 3) A. J. Farmer and E. S. Phinney, *Mon. Not. R. Astron. Soc.* **346** (2003), 1197.
- 4) M. V. Sazhin, *Sov. Astron.* **22** (1978), 36.
S. Detweiler, *Astrophys. J.* **234** (1979), 1100.
- 5) F. A. Jenet, G. B. Hobbs, K. J. Lee and R. N. Manchester, *Astrophys. J.* **625** (2005), L123.
- 6) G. Hobbs, *Publ. Astron. Soc. Australia* **22** (2005), 179.
- 7) S. Mikkola and M. J. Valtonen, *Mon. Not. R. Astron. Soc.* **259** (1992), 115.
- 8) T. Fukushige, T. Ebisuzaki and J. Makino, *Publ. Astron. Soc. Japan.* **44** (1992), 281.
- 9) M. Iwasawa, Y. Funato and J. Makino, *astro-ph/0511391*.
- 10) T. Matsubayashi, J. Makino and T. Ebisuzaki, *astro-ph/0511782*.
- 11) P. J. Armitage and P. Natarajan, *Astrophys. J.* **634** (2005), 921.
- 12) P. C. Peters and J. Mathews, *Phys. Rev.* **131** (1963), 435.
P. C. Peters, *Phys. Rev.* **136** (1964), 1224.
- 13) M. Fitchett, *Mon. Not. R. Astron. Soc.* **224** (1987), 567.
- 14) E. S. Phinney, *astro-ph/0108028*.
- 15) M. Nagashima, T. Totani, N. Gouda and Y. Yoshii, *Astrophys. J.* **557** (2001), 505.
M. Nagashima, Y. Yoshii, T. Totani and N. Gouda *Astrophys. J.* **578** (2002), 675.
- 16) M. Enoki, M. Nagashima and N. Gouda, *Publ. Astron. Soc. Japan.* **55** (2003), 133.
- 17) A. N. Lommen, *in MPE Rep. 278, WE-Heraeus Seminar on Neutron Stars, Pulsars and*

Supernova Remnants, (eds W. Becker, H. Lesch & J. Truemper, Garching:MPE, 2002).

- 18) F. A. Jenet, et al., accepted by *Astrophys. J.*, astro-ph/0609013.
- 19) P. Salucci, E. Szuszkiewicz, P. Monaco and L. Danese, *Mon. Not. R. Astron. Soc.* **303** (1999), 637.